Check for updates

# Tear of lipid membranes by nanoparticles†‡

Mériem Er-Rafik,*[ab] Khalid Ferji, [ID] *[cde] Jérôme Combet,[a] Olivier Sandre, [ID] [cd]
Sébastien Lecommandoux, [ID] [cd] Marc Schmutz, [ID] [a] Jean-François Le Meins [ID] [cd]
and Carlos M. Marques [ID] ‡*[a]

**Health concerns associated with the advent of nanotechnologies
have risen sharply when it was found that particles of nanoscopic
dimensions reach the cell lumina. Plasma and organelle lipid mem-
branes, which are exposed to both the incoming and the engulfed
nanoparticles, are the primary targets of possible disruptions.
However, reported adhesion, invagination and embedment of
nanoparticles (NPs) do not compromise the membrane integrity,
precluding direct bilayer damage as a mechanism for toxicity. Here
it is shown that a lipid membrane can be torn by small enough
nanoparticles, thus unveiling mechanisms for how lipid membrane
can be compromised by tearing from nanoparticles. Surprisingly,
visualization by cryo transmission electron microscopy (cryo-TEM)
of liposomes exposed to nanoparticles revealed also that liposomal
laceration is prevented by particle abundance. Membrane destruc-
tion results thus from a subtle particle-membrane interplay that is
here elucidated. This brings into a firmer molecular basis the
theorized mechanisms of nanoparticle effects on lipid bilayers
and paves the way for a better assessment of nanoparticle toxicity.**

Frequent contact between particles of nanoscopic dimensions
and the lipid membranes of living organisms is an ineluctable
consequence of the rising abundance of nanoparticles in
modern technological applications.[1,2,3] The fate of such con-
tacts between particles and membranes, whether accidental or
purposeful, is arguably a key determinant to evaluate levels of
nano-toxicity or the efficiency of strategies for nano-therapy.
But a decade of scrutiny of the transformations induced by
nanoparticles on model lipid membranes has only reported
mild consequences for the bilayers,[4–7] see also ref. 8 for a
review of the field. For hydrophilic particles, moderate affinity
for the membrane surface leads to attachment to the outer
membrane leaflet, in a partially wrapped state.[9] For larger
adhesion energies wrapping becomes complete and the particle
is invaginated from the outer to the inner side of the exposed
membrane.[10] In a liposome, this leads to a final structure
where the particle has crossed the membrane barrier into the
liposome lumen in a wrapped – thus protected – state.[5] Hydro-
phobic particles can either stay embedded in the inner bilayer
or, when properly decorated, cross from one side to the other,[7]
a process referred to as translocation. In all cases, the
membrane is left undisturbed.

In the quest for unveiling the conditions under which the
interaction between nanoparticles and membranes might lead
to severe membrane disruption, we investigated colloidal sus-
pensions containing liposomes of DOPC, a zwitterionic lipid
forming liquid-phase bilayers of 5 nm thickness,[11] and SiO$_2$
nanoparticles of comparable radii. At such small particle
dimensions it is foreseen that, if wrapping occurs, membrane
deformations will be pushed well beyond their elastic deforma-
tion limit, thus increasing the likeness of irreversible
membrane damage.

Fig. 1 displays cryo-TEM images of SiO$_2$ nanoparticles, of
DOPC liposomes and their mixtures at a ratio of five nano-
particles per liposome at pH 5.5 and 10 mM of KCl, along with a
schematic representation of the typical features observed as
one increases the time lapse after the nanoparticles have been
added to the liposome suspension. As Fig. 1A shows, the SiO$_2$
nanoparticles are round-shaped, albeit not perfectly spherical.
Their average diameter is 12.2 ± 1.7 nm, as determined from
the mean and the standard deviation of the size distribution,
also displayed in the figure, sampled from over one hundred
particles. Comparable dimensions were also obtained from
small angle X-ray scattering (SAXS) experiments of particle

$^a$ *Institut Charles Sadron, Université de Strasbourg, CNRS-UPR 22, 23 rue du Loess,
67034 Strasbourg Cedex 02, France. E-mail: marques@unistra.fr*

$^b$ *C-Cina, BioEMLab, Biozentrum, Mattenstrasse 26, CH-4058 Basel, Switzerland.
E-mail: meriem.er-rafik@unibas.ch*

$^c$ *University of Bordeaux, LCPO UMR 5629, 16 avenue Pey Berland, F-33600 Pessac,
France*

$^d$ *CNRS, LCPO UMR 5629, 16 avenue Pey Berland, F-33600 Pessac, France*

$^e$ *Ecole Nationale Supérieure des Industries Chimiques, Laboratoire de Chimie
Physique Macromoléculaire, 1 rue Grandville BP20451, 54000 Nancy, France.
E-mail: khalid.ferji@univ-lorraine.fr*

† Electronic supplementary information (ESI) available. See DOI: **https://doi.org/
10.1039/d2sm00179a**

‡ Current address: Université de Lyon, ENS Lyon, CNRS UMR 5182, Laboratoire
de Chimie, 46 Allée d'Italie, 49634 Lyon, France.
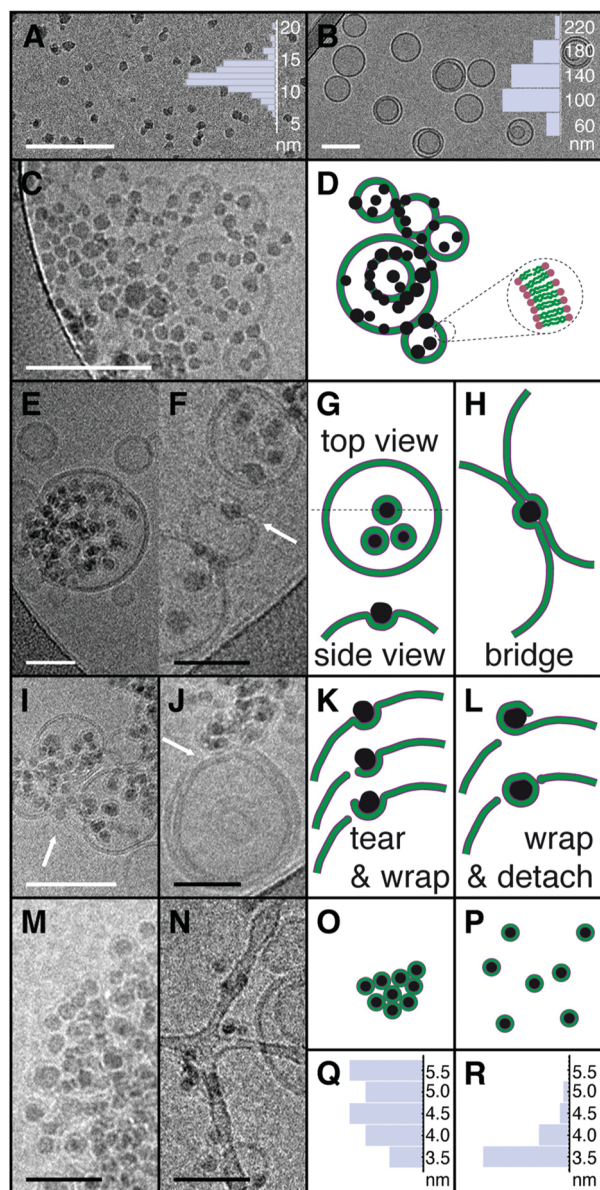
**Fig. 1** Cryo-TEM images of SiO$_2$ nanoparticles (SM30 Ludox®) and DOPC liposomes at nanoparticles per liposome ratio $r$ = 5 with corresponding schema highlighting the relevant interaction aspects. (A) Image of the SM30 particles in a dilute brine solution of 10 mM KCl and the associated diameter distribution with average diameter 12.2 ± 1.7 nm. (B) Image of the DOPC liposomes in 10 mM KCl. Liposome diameter distribution is also represented with average diameter 125 ± 34 nm. (C) Image of a NP/liposome mixture, 20 seconds after the nanoparticles have been added to the liposome solution. (D) Schematic representation of a chosen area in the C image. The particles are shown in black, while the membranes are displayed as a hydrophobic tail layer in green and a hydrophilic head region in purple. All the particles are in contact with the lipid bilayer. (E and F) Images of the NP/liposome suspension one minute after mixing. (G) Top and side views of the NPs partially wrapped by the membrane of the larger liposome in E. (H) A schematic illustration of the interaction topology in image F where one particle bridges the bilayers from two neighbor liposomes. (I and J) Images after 30 minutes of NP/liposome contact. (K) Schematic representation of the tearing event pointed by the arrow in figure I, caused by a NP which is not yet completely wrapped by the lipid bilayer. (L) Schematics of a NP completely wrapped following the tearing event shown in image J. (M and N) The NP/membranes systems respectively

two and four months after mixing. (O) The scheme of image M shows NPs completely wrapped by the bilayer membrane. Here, the NPs are not yet dispersed. (P) Fully wrapped and dispersed NPs as shown in image N. (Q) Thickness distribution of the bilayers from liposomes not exposed to NPs, showing an average thickness of 4.7 ± 0.5 nm measured from head to head. (R) Thickness distribution of the bilayers completely wrapping the nanoparticles from four months old samples, with an average thickness of 3.7 ± 0.3 nm measured from the head position far from the silica surface to the tail-head interface on the silica surface. White scale bar 100 nm, black scale bar 50 nm.

suspensions, see ESI† Fig. S1. A typical image of the DOPC liposomes, shown in Fig. 1B, confirms that our preparation method yields a majority of unilamellar structures, with a fraction of multilamellar liposomes. The liposome size distribution, also presented in the figure, provides values for average size and mean deviations at 125 ± 34 nm. Size distributions from measurements of the bilayer thickness, displayed in Fig. 1Q, yields 4.7 ± 0.5 nm, in agreement with literature values.[11,12] Comparable conclusions can be drawn from small angle neutron and X-ray scattering, SANS and SAXS, as well as from static and dynamic light scattering, SLS and DLS, as displayed in the Fig. S1 and S9 (ESI†). Under our conditions, the attractions between the nanoparticles and the liposomes result in a fast attachment. Fig. 1C shows an image of the system 20 s after the NPs have been added to the liposome suspension. As the image and its corresponding schematic representation in Fig. 1D show, all the NPs are found to be in contact with the liposome bilayers, albeit with little development yet of wrapping, a feature that is associated with the majority of NP-membrane contacts in the samples imaged later, one minute after addition of the NPs. Typical images of such samples are shown in Fig. 1E and F with the corresponding schematic representations displayed in Fig. 1G and H. At this stage, most of the NPs have been partially wrapped by the lipid bilayer, a typical situation consisting in membrane wrapping of about a half of the NP surface, which can be perceived from both top and side views of the membrane deformations around the particles. Note that top views alone cannot discriminate between partial wrapping and particle engulfment by the liposome. In our case, we confirmed that engulfment does not occur by imaging tilted samples under the electron beam. Partial wrapping results also in the presence of bridges between the membranes of different liposomes, a situation depicted in Fig. 1H. Partial wrapping is not however the final equilibrium state resulting from NP-membrane interactions. As Fig. 1I and J show, exposure of the membranes to the NPs over a period of 30 minutes results in many events where the membrane is torn by the nanoparticles. The sequence of tear formation can be deduced by careful inspection of the micrographs as summarized in Fig. 1K and L. In a first step, that we call tear and wrapping, a partially wrapped NP lacerates the membrane in a localized incision, allowing further wrapping to occur by the membrane to which the NP stayed attached. Continuation of this process results in a complete covering of the NPs and the consequent detachment of a fully wrapped particle from the membrane. We call this step

"wrapping and detach". Observation of the membrane and NP system over longer period of times confirms the destruction potential of these interactions as unwrapped NPs can no longer be observed in the micrographs. After two months, all the NPs are protected by a phospholipid bilayer, the dominant spatial distribution exhibiting many bunches of NPs, see Fig. 1M and O. This long-time, slow evolution eventually leads after four months to a suspension of fully wrapped NPs well dispersed in the suspension as shown in Fig. 1N and P. At this point, measurement of the thickness of the membranes wrapping the NPs reveals that the thickness of the attached bilayers is comparable to that of free liposomes. The difference of 1 nm between the mean values in the histograms of Fig. 1Q and R being due to the missing head region in contact with the silica surface that cannot be captured by the electronic contrast. Note that images presented here are representative of phenomena observed in several tens of images from independent experiments performed at least three times for each condition.

Analysis of cryo-TEM images and the scattering experiments described in the ESI† – that as we will describe below, fully support cryo-EM evidence – provides thus a clear scenario for the sequence of events and for the key factors leading to membrane tear and to the ensuing membrane destruction. As a prime factor, a strong attraction between the NPs and the lipid bilayer is at play in this system. While in pure NP colloidal solutions the particles are mostly seen as single particles, well dispersed with minor degree of aggregation, for all the suspensions containing NPs and membranes the images show, at any stage of the mixture, that all NPs have adhered to a bilayer. The major direct consequence of this affinity is the deformation of the membrane as it progressively wraps around the NPs. Membrane deformations are also known to mediate attractive interactions between the adhered NPs.[13,14] Here, such attractions are clearly evidenced by the numerous particle–particle contacts seen in the micrographs, often resulting in pearl-like arrangements of NPs. As the membrane progressively wraps around the NPs a point is reached where the membrane is torn at the triple contact line between the free membrane, the adhered membrane and the free particle surface. Wrapping proceeds then further until a fully covered NP detaches from the bilayer. The long-term consequence is complete wrapping of all particles.

Our results show that less than 20 seconds are required for all NPs to encounter and bind to the membranes, a short time compatible with a diffusion limited mechanism for the adhesion between NPs and liposomes. Indeed, under our conditions, the diffusion time of a NP of 10 nm diameter over a typical distance between liposomes ($\sim$ 500 nm) is smaller than one second. Also, the first images at 20 seconds already exhibit particle organization at the membrane surface, showing that the development of the membrane deformation fields and the consequent membrane-mediated interactions between the particles occur on fast time scales. However the steps that led to further particle wrapping and eventually to membrane rupture are much slower. Further wrapping requires of order of one minute, rupture is only seen after tens of minutes and several
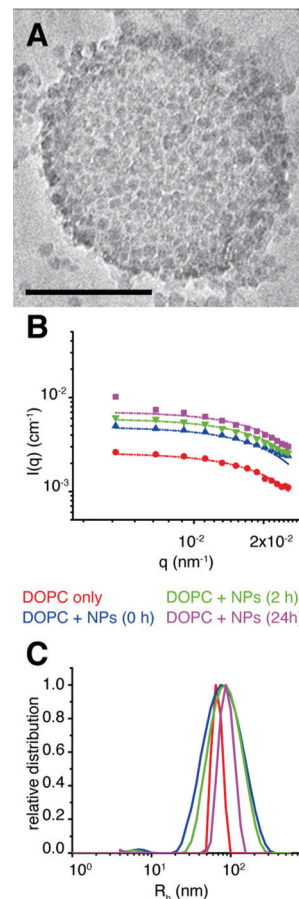


Fig. 2 Large nanoparticle per liposome ratios $r$ stabilize the membranes. (A) Cryo-TEM image of a NP/liposome mixture with $r = 50$, one minute after the nanoparticles have been added to the liposome solution, scale bar 100 nm. All particles adhere to the liposomes, without any visible membrane disruption. (B) Light scattering spectrum from a mixture of $r = 280$ at different stages after mixing and (C) the corresponding size distribution from DLS measurement of the same systems.

months are necessary to completely enwreathe all the NPs and destroy the membranes completely. Such large time scales can only be understood by long-lived phenomena, such as the collective lipid rearrangement that would be required for significant membrane thinning.

A combination of factors contributes to the membrane rupture. Most strikingly, the radii of the NPs are comparable to the bilayer thickness. Wrapping leads thus to high bending, a deformation state that imposes strong stresses in the two leaflets of the bilayer. The middle plane of the hydrophobic region of the outer leaflet, located at a distance of 3.5 nm from the NP surface is stretched by 13% with respect to the middle bilayer plane at 2.5 nm. For uniform stretching, lysis of the DOPC bilayer is known to occur above membrane tensions of the order of a few mN m$^{-1}$, at deformations between 5% and 10%.[11] For the upper bound of 10%, this simple argument would predict that NPs with radii below 7.5 nm can induce large enough stresses to rupture the bilayer. For our case, the combined effect of the adhesion forces and the curvature generates thus a wrapped bilayer state that is close to the
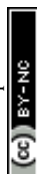
rupture point. Maximal gradients of bilayer properties are obviously located at the triple contact line, where imposed stresses overcome membrane cohesive forces when, according to our estimation, the angle between the membrane and the particle surface exceeds 90°, the point of half wrapping. That a minimal angle is required to rupture the membrane is confirmed in a strikingly manner by experiments performed with a high particle to liposome ratio $r$, see Fig. 2 and Fig. S2 (ESI†).

To investigate the influence of the electrostatic charge on the liposome–NP interaction experiments were performed under the same conditions (ratio of five NP per liposome, 10 mM KCl) but with different pH (7 and 10). These experiments (see Fig. S2, ESI†) gave results comparable to those performed at pH 5.5. Also, experiments performed at pH 5.5 without KCl showed that the presence of 10 mM KCl has no effect in the tearing-wrapping mechanism (Fig. S3, ESI†). Moreover, at pH = 5.5 and 10 mM KCl, the zeta potential of Silica NPs and DOPC liposome was measured at −21 mV and −6 mV respectively. After the mixture of Silica NPs and DOPC liposomes, the zeta potential was reduced to −8 mV, a reduction likely to be due to the decoration of the silica NP particles by the lipid membrane. The most standard explanation of the attractive interactions between the zwitterionic lipids and the silica surface involves the attractions between the silanol groups on the silica surface and the quaternary amines of the lipid heads as described in the literature.[15]

For all the ratios explored here, $r = 50$, $r = 140$ and $r = 280$ no membrane rupture was detected, despite the strong coverage of the membranes by the NPs, see also Fig. S4–S6 (ESI†). This apparently counterintuitive result obtained by increasing only the ratio of NP to liposomes, can be rationalized in the following way. Simple geometric considerations show that a NP of 5 nm radius requires 0.5% of the area of a 50 nm radius liposome to be half wrapped. Since it is unlikely that liposomes possess more than 5 or 10% of excess available area, angles of the triple line as large as 90° cannot be achieved if more than 10 or 20 NPs are attached to the membrane. In our case, amongst all the ratios tested, experiments (not shown) with $r = 8$ was the largest still leading to membrane tearing. Note that preservation of membrane integrity does not imply that membrane properties are kept unchanged, and we anticipate that in further studies of these systems reminiscent of Pickering emulsions one is likely to find that NP coverage leads to significant modifications of membrane mechanics and permeability.

We stress that the scenario put forward above from the observation of tens of EM images is fully supported by data from multi-angle light scattering, a technique that probes trillions of liposomes simultaneously, see ESI† for a complete description. In brief, at high nanoparticles per liposome ratio ($r = 280$), the whole scattering profile increases with little change of the form factor (Fig. S9A, ESI†), consistent with the formation of liposomes decorated by attached NPs. At intermediate ratios ($r = 140$ and $r = 50$), cluster formation is observed as evidenced by the strong upturn of the curves towards low scattering vectors (Fig. S9B and C, ESI†). Finally, at $r = 5$, the whole scattering curve decreases, a loss of scattering ascribed to the disruption of a large fraction of liposomes into much smaller objects (Fig. S9D, ESI†).

As a summary, we reported here evidence for lipid bilayer tearing by $SiO_2$ NPs of 12 nm diameter and identified strong adhesion, high curvature and a large degree of wrapping as the key factors that compromise membrane integrity. We expect these key results to hold across a variety of more complex membrane systems and NPs suspensions, and in particular to provide useful guidelines for the evaluation of NPs toxicity in biological systems.

## Experimental section

### Chemicals and materials

DOPC, (1,2-dioleoyl-$sn$-glycero-3-phosphocholine) was purchased from Avanti Polar Lipids Inc. and has been used to form LUVs. Ludox® SM colloidal silica nanoparticles were purchased from Sigma-Aldrich.

### Sample preparation

Vesicles were prepared by the sonication method, using the protocol described in the ESI.† In order to disperse the NPs, the solution was sonicated in the bath for 15 min before added to DOPC vesicles. The SM30 NPs initial concentration obtaining isolated NPs have been determinate by cryo-TEM and SAXS analyses.

### Cryo-transmission electron microscopy (cryo-TEM)

Images were taken at room temperature from vitrified samples. Sample vitrification was carried out in a homemade vitrification system. The samples were observed under low dose conditions in a Tecnai G2 microscope (FEI) at 200 kV. Images were acquired using an Eagle slow scan CCD camera (FEI). To check inner liposome content some images were observed at different tilting angles by tilting the cryo-holder. The size distribution of the NPs, the lipid vesicle diameter and the membrane thickness were measured with the Analysis software (SIS-Olympus, Münster, Germany). The size of NPs and lipid vesicles were determined with the circular shape predefined by the software. The membrane thickness of the lipid vesicle and the one surrounded the NPs were determined by a horizontal density profile. Membrane thickness was measured for the free liposomes between the darkest values of the radial grayscale profiles, which corresponds to the distance between the lipid heads. For the bilayers attached to the particles the head region in contact with the silica is not visible, the distance was measured between the external heads (darkest external value of the grayscale profile) and the end of the internal hydrophobic leaflet (last light greyscale level of the profile). Differences between both methods are of order of 1 nm, the thickness of the head region. For each experiment, the diameters and the membrane thicknesses of more than 60 liposomes and 170 NPs were measured and averaged.

## Conflicts of interest

There are no conflicts to declare.

## Acknowledgements

## References

1 N. Lewinski, V. Colvin and R. Drezek, *Small*, 2008, **4**, 26.

2 M. P. Stewart, A. Sharei, X. Ding, G. Sahay, R. Langer and K. F. Jensen, *Nature*, 2016, **538**, 183.

3 A. E. Nel, L. Mädler, D. Velegol, T. Xia, E. M. Hoek, P. Somasundaran, F. Klaessig, V. Castranova and M. Thompson, *Nat. Mater.*, 2009, **8**, 543.

4 R. Michel, T. Plostica, L. Abezgauz, D. Danino and M. Gradzielski, *Soft Matter*, 2013, **9**, 4167.

5 O. Le Bihan, P. Bonnafous, L. Marak, T. Bickel, S. Trépout, S. Mornet, F. De Haas, H. Talbot, J. C. Taveau and O. Lambert, *J. Struct. Biol.*, 2009, **168**, 419.

6 R. Michel, E. Keeselman, T. Plostica, D. Danino and M. Gradzielski, *Angew. Chem., Int. Ed.*, 2014, **53**, 12441.

7 Y. Guo, E. Terazzi, R. Seemann, J. B. Fleury and V. A. Baulin, *Sci. Adv.*, 2016, **2**, e1600261.

8 E. Rascol, J. M. Devoisselle and J. Chopineau, *Nanoscale*, 2016, **8**, 4780.

9 S. Zhang, A. Nelson and P. A. Beales, *Langmuir*, 2012, **28**, 12831.

10 K. Jaskiewicz, A. Larsen, D. Schaeffel, K. Koynov, I. Lieberwirth, G. Fytas, K. Landfester and A. Kroeger, *ACS Nano*, 2012, **6**, 7254.

11 D. Marsh, *Handbook of lipid bilayers*, CRC Press, Boca Raton, FL, USA, 2013.

12 J. Lepault, F. Pattus and N. Martin, *Biochim. Biophys. Acta, Biomembr.*, 1985, **820**, 315.

13 I. Koltover, J. O. Raedler and C. R. Safinya, *Phys. Rev. Lett.*, 1999, **82**, 1991.

14 M. M. Müller, M. Deserno and J. Guven, *Phys. Rev. E: Stat., Nonlinear, Soft Matter Phys.*, 2005, **72**, 061407.

15 H. Kettiger, G. Québatte, B. Perrone and J. Huwyler, *Biochim. Biophys. Acta, Biomembr.*, 2016, **1858**, 2163.